

Supporting Information

Determination of Aflatoxin M1 using aptamer based biosensor on the surface of dendritic fibrous nano-silica functionalized by amine groups

Houman Kholafazad kordasht ^a, Mohammad hasanzadeh ^{b*}, Mir-Hassan Moosavy ^{a**}, Jafar Soleymani ^c, Ahad Mokhtarzadeh ^e

^a Department of Food Hygiene and Aquatics, Faculty of Veterinary Medicine, University of Tabriz, Tabriz, Iran.

^b Drug Applied Research Center, Tabriz University of Medical Sciences, Tabriz, Iran.

^c Pharmaceutical Analysis Research Center, Tabriz University of Medical Sciences, Tabriz, Iran.

^d Department of Nanochemistry, Nanotechnology Research Center, Uremia University, Uremia, Iran.

^e Immunology Research Center, Tabriz University of Medical Sciences, Tabriz, Iran.

Corresponding Author

E-mail address: (*) hasanzadehm@tbzmed.ac.ir

(**) mhmoosavy@gmail.com

3.1. GQDs and GQDs-CS synthesis and characterization

GQDs and GQDs-CS were synthesized according to our previous work [1, 2]. An easy bottom-up method was used for the preparation of GQDs. At first, GQDs were synthesized by pyrolyzing citric acid and dispersing the carbonized products into alkaline solutions. Briefly, 2 g of citric acid was put into a beaker and heated to 200 °C by a heating mantle until the citric acid changed to an orange liquid. Then, for preparing GQDs, 100 mL of 10 mg/mL NaOH solution was added into the orange homogenous liquid dropwise with continuous stirring. The obtained GQD solution was stable for at least one month at 4 °C and in GQDs-CS synthesis, CS solution (2 g. L⁻¹) was prepared by dissolving CS in 0.1 M acetic acid, and then the yellow GQDs aqueous solution (2 g. L⁻¹) was added into the CS solution under stirring. After 10 min of stirring, the mixture was adjusted by addition of 10% (w/w) sodium hydroxide solution dropwise. The precipitate was washed with ultrapure water several times to remove the residual impurities, and the obtained GQDs-CS were freeze dried in a lyophilizer at -40 °C for 24 h. The GQDs toxicity was evaluated in previous research on NIH-3T3 and HepG2 cells, so these cells were exposed to different concentrations of GQD (0, 10, 20, 50, 100 and 200 ppm) for 24, 48 and 72 hours [1]. As a result, increasing doses of GQD up to 200 ppm, do not have any striking result on cell viability by MTT.

FT-IR, DLS, Zeta potential analysis, XRD and AFM were used for the characterization of GQD and GQDs-CS nanocomposites. By FT-IR, the surface chemistry of GQDs and CS-GQDs were investigated. The FT-IR spectrum of GQDs and GQDs-CS nanocomposites are shown in (Fig. S1A) and that spectrum about GQDs showed two main peaks at 1716 cm⁻¹ and 1766 cm⁻¹ and these are assigned to the stretching vibrations of C=O from the -COOH groups. For GQDs-CS, two peaks at 1604 and 1766 cm⁻¹ are related to strong electrostatic attraction between CS and GQDs. Furthermore, the C=O stretching of GQDs is reduced from 1716 to 1708 cm⁻¹, which can be arising from the formation of H-bonding inside the nanocomposites.

The DLS study result showed a growth in the particle size of the GQDs-CS that accepted via zeta potential analyses (Fig. S1B). The result shows that CS was successfully attached to GQDs structure, which caused the negative zeta potential value to change to more negative potentials and where the negative charge has a major effect in the stability of GQDs-CS (Fig. S1C).

XRD patterns were checked on a Siemens D 5000 X-Ray diffractometer (Texas, USA) with a Cu K α anode ($\lambda = 1.54 \text{ \AA}$) operating at 40 kV and 30 mA. The diffraction patterns were collected at 25 °C and over an angular range of 3.0 to 10 and 10 to 70° with a dwell time of 12 s per increment and step size of 0.05° per step (Fig. S1D). For more confirmation, the morphology of GQDs and GQDs-CS were characterized by AFM image (Fig. 1E).

3.2. Synthesis and characterization of KCC-1-NH₂-Tb

The KCC-1 synthesis follows a generic synthesis [3]. Briefly, tetraethyl orthosilicate (TEOS, 2.5 g, 0.012 mol) was dissolved in a solution of cyclohexane (30 mL) and pentanol (1.5 mL) and then a stirred solution of cetylpyridinium bromide (CPB; 1 g, 0.0026 mol) and urea (0.6 g, 0.01 mol) in water (30 mL) was then added. Fig. S2A is TEM images of KCC-1 and that is confirmed successful synthesis of this material. For the synthesis of KCC-1-NH₂, 20 ml THF and 2 mmol of KCC-1 were combined together and the next 20 mmol of NaOH was dispersed in to the mixture by sonication [4]. 22 mmol of 3-aminopropyltriethoxysilane (APTES) was added drop by drop at room temperature and stirred for another 16 h at 60 °C. The acquired products were collected and washed with deionized water and ethanol in sequence and afterward dried action has done under vacuum at 60 °C for 2 h for further use. Scheme 1 was summarized all of the synthesis procedure. The TEM images of KCC-1-NH₂ has showed in (Fig. S2B). For the KCC-1-NH₂-Tb synthesis 1 g CTAB, 225 g water and 3.5 ml NaOH were mixed together. Then 55.5 ml TEOS and 15 ml of Tb⁺³ were added. The mixture was incubated at 20 °C for 2 h. then the composite washed with ethanol and water. The drying

process was done at the room temperature in the vacuum. The comparison TEM images of the KCC-1 and KCC-1-NH₂ show that the structure is similar, but the KCC-1-NH₂-Tb morphology is amorphous (Fig. S2). On the other hand, investigation of the agglomeration and local accumulation only indicate low agglomeration of KCC-1-NH₂-Tb. According to Fig. S4, the structure form of these compounds are dendritic spheres with uniform structure. The images clearly illustrated that these materials possess dendritic fibers orderly in three dimensions to form spheres, which may let effortless access to the available high surface area.

The XRD analysis (Fig. S5) demonstrate two peak centered at around 11° and 22° in both KCC-1 and KCC-1-NH₂, respectively. Also KCC-1-NH₂-Tb has wide peak centered at around 22°.

The specific surface area and porosity of the materials were determined using the adsorption isotherm and calculated by BET. Also, BJH method was used to determine the pore volume of the KCC-1, KCC-1-NH₂ and KCC-1-NH₂-Tb. Table S1 lists the average pore size, surface area and pore volume of KCC-1, KCC-1-NH₂ and KCC-1-NH₂-FA. The BJH pore volumes were changed from 1.52 to 1.1 and 1.01 cm³/g for KCC-1, KCC-1-NH₂ and KCC-1-NH₂-Tb and surface area of KCC-1 changed from 617 m²/g to 367 and 633 m²/g for KCC-1-NH₂ and KCC-1-NH₂-Tb, respectively. Mean pore diameter distribution of the materials were 9.9, 11.9 and 6.94 for KCC-1, KCC-1-NH₂ and KCC-1-NH₂-FA, respectively (Fig. S6). The pore size, pore volumes and surface area of KCC-1, KCC-1-NH₂ and KCC-1-NH₂-Tb are obviously confirmed by the previously reported results.

Functional groups of the synthesized materials was characterized by FTIR. As shown in Fig. S7, the characteristic peaks of the silica based materials could be observed in the range of 1020 to 1110 cm⁻¹ representing the Si-O-Si asymmetric stretching and Si-OH peak is observed at 960 cm⁻¹ which represents the stretching vibration and asymmetric bending. Also, the peak at around 1500 cm⁻¹ is assigned to the Tb and KCC-1-NH₂.

The DLS study indicated that particle size of KCC-1-NH₂ was increased, but the KCC-1-NH₂-Tb particle size is almost similar (Fig. S8). The toxicity of KCC-1-NH₂-Tb was investigated by MTT assay on HT 29 cancer cell lines in the different concentration (1, 10, 20, 50, 100 and 150 ppm) for 24, 48 and 72 h. The result show that the KCC-1-NH₂-Tb is not toxicity material (Fig. S9).

3.3. Electrodeposition of GQDs-CS and KCC-1-NH₂-Tb

Before start experiment, the GCE was polished for having reliable and repeatable responses. In this regard, polishing was done with 0.05 μm alumina (Beuhler, USA) powder on the standard pad, afterward the GCE was ultrasonically rinsed steadily with 1:1 alcohol, acid nitric and water. Finally it allowed to dry at room temperature [5]. Covering of GCE surface is extremely momentous step in the design of the biosensor. For this purpose, electrochemical deposition of GQDs-CS on the surface of GCE was done and that show in (Fig. S10.A). The electrochemical deposition was started, when GCE located in in the cell containing 10 mL of CS-GQDs and that procedure was manufactured via CV with 30 consecutive cycles in the potential range of 0 to 1 V vs. Ag/AgCl. Also, -NH₂ groups of CS at the C-2 position of the D-glucopyranose repeating unit could be protonated in the acidic media [25, 26]. On the other hand, the result of GQDs dispersed in water has extremely negative charge. So ionization of oxygen containing functional groups (mainly-COOH) on the structure of GQDs, which is favor of their composition with positively charged CS. In addition, the zeta potentials result, prove GQDs have negatively charged (-10 mV) and CS with NH₃⁺ groups is positively charged (+65 mV). The -NH₃⁺ groups on CS chip has electrostatic attraction with dominant -COO- groups of GQDs. Hence, there also exist vast H-bindings between-OH groups on the surface of GQDs and -CO₂H groups of CS. H- bonding and both electrostatic attraction persuade interfacial adhesion of GQDs and CS, lead to formation of homogeneous nanocomposites of GQDs-CS. At the second step, KCC-1-NH₂-Tb was electrodeposited on the surface of GQDs-

CS using CHA techniques at the $E=-0.24V$ and duration time of 500 s (Fig. s10.B). KCC-1-NH₂-Tb have negative.

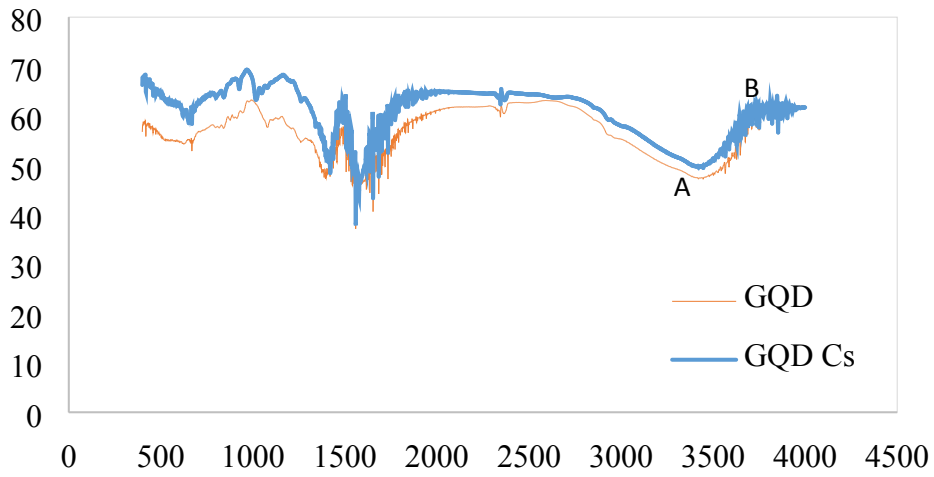
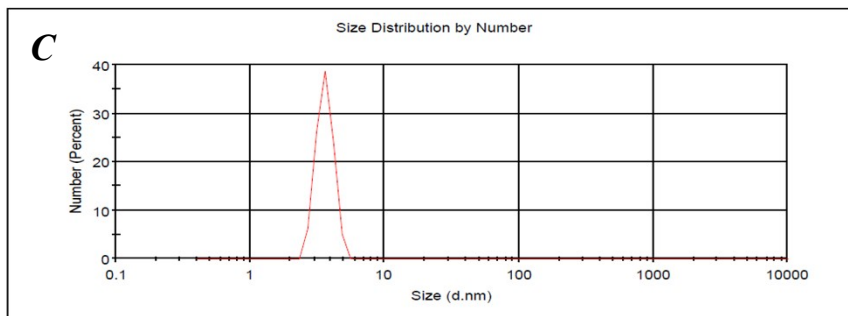


Fig. 1. A

	Size (d.n...	% Number:	St Dev (d.n...
Z-Average (d.nm): 1946	Peak 1: 3.628	100.0	0.5231
Pdl: 0.865	Peak 2: 0.000	0.0	0.000
Intercept: 0.568	Peak 3: 0.000	0.0	0.000

Result quality Refer to quality report



	Size (d.n...	% Number:	St Dev (d.n...
Z-Average (d.nm): 2802	Peak 1: 3269	100.0	848.3
Pdl: 0.295	Peak 2: 0.000	0.0	0.000
Intercept: 0.873	Peak 3: 0.000	0.0	0.000

Result quality Refer to quality report

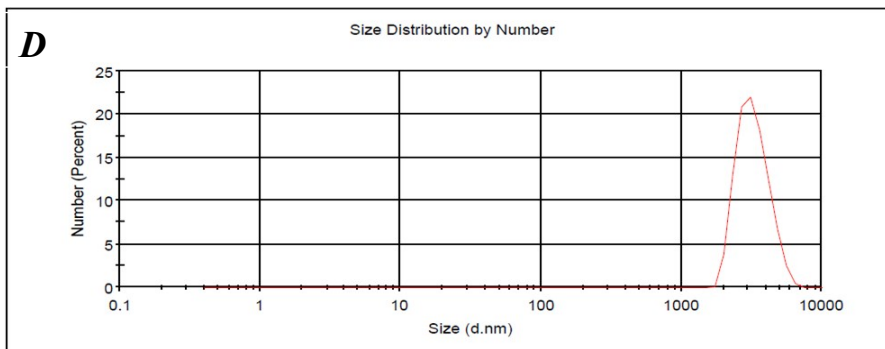
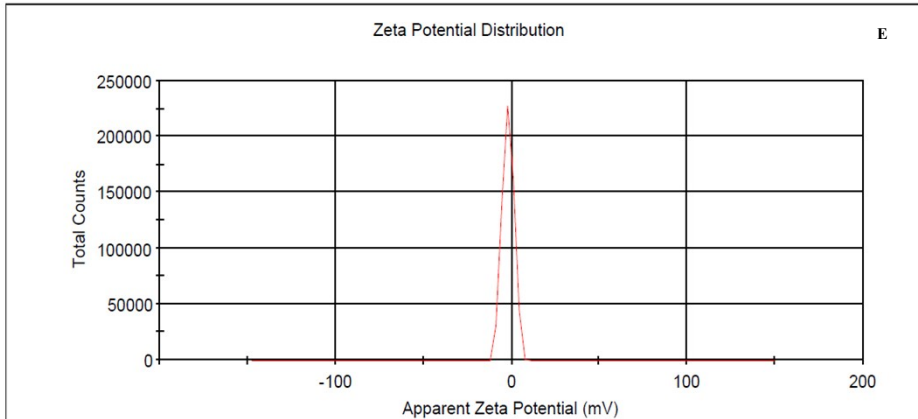
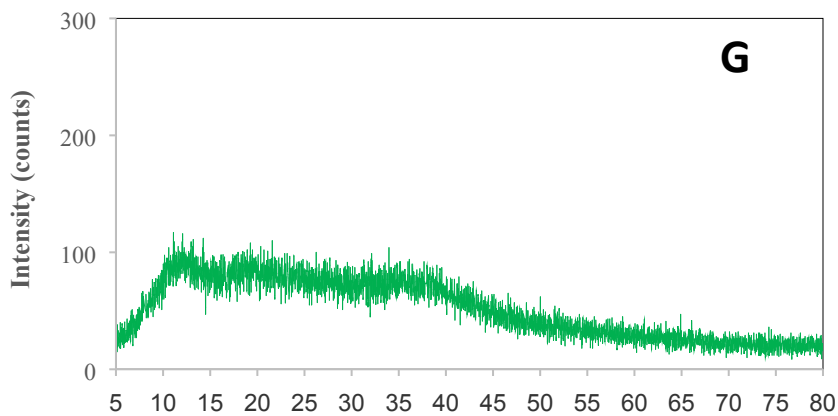
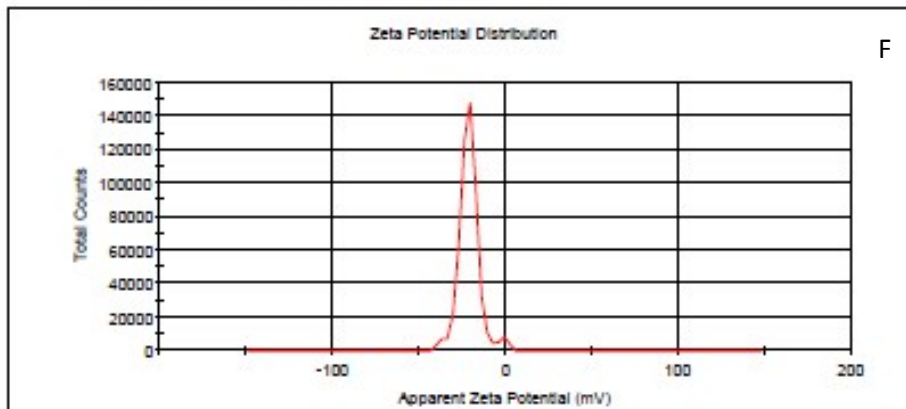


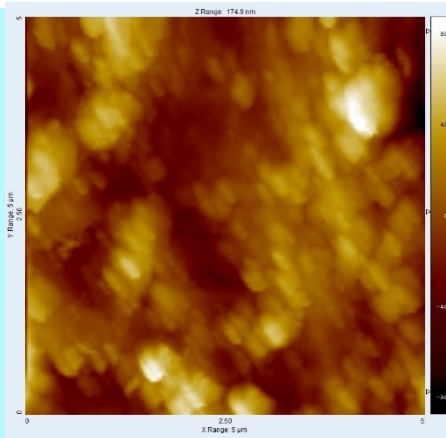
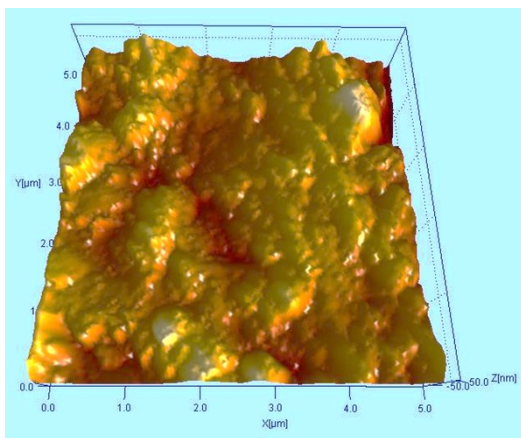
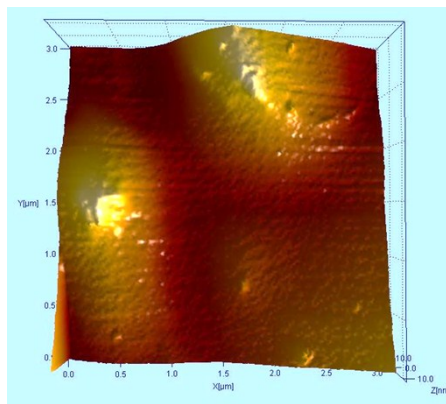
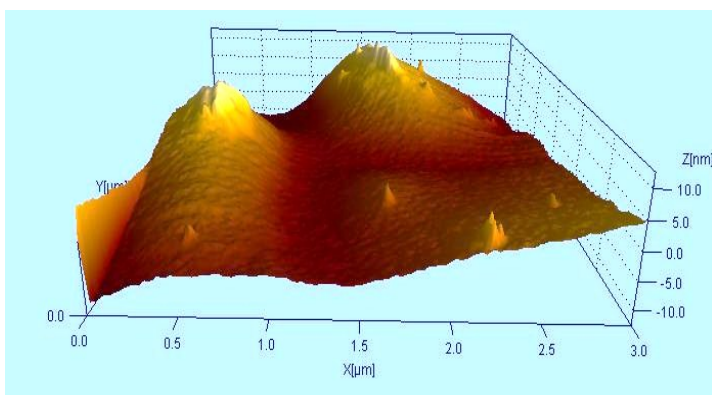
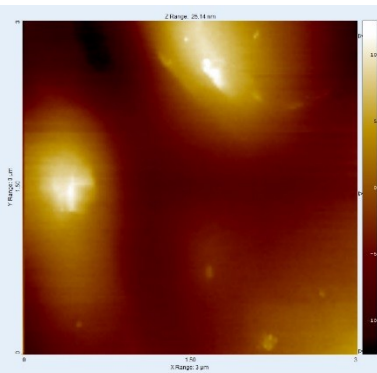
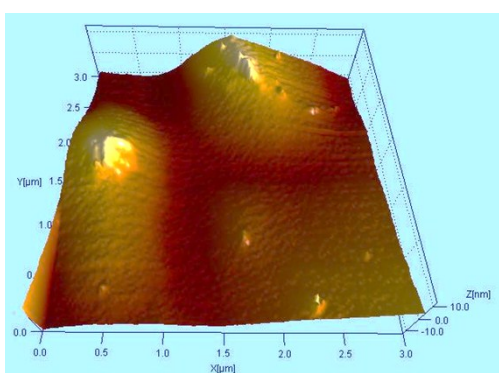
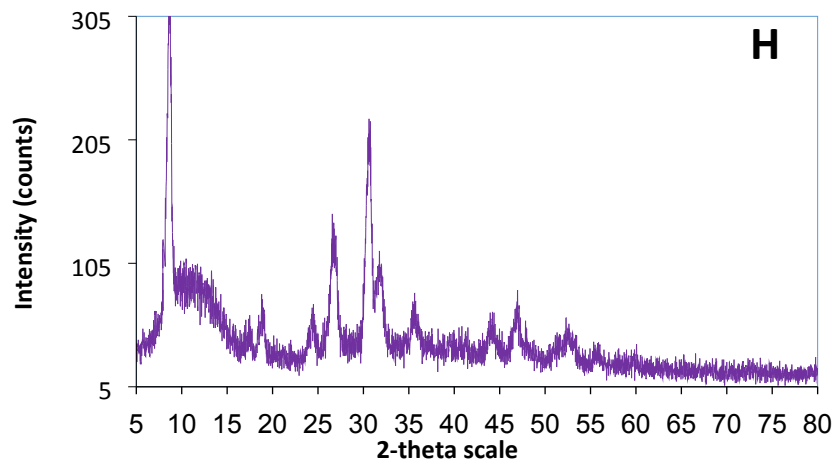
Fig. 1. B

	Mean (mV)	Area (%)	St Dev (mV)
Zeta Potential (mV): -1.87	Peak 1: -1.87	100.0	3.32
Zeta Deviation (mV): 3.32	Peak 2: 0.00	0.0	0.00
Conductivity (mS/cm): 0.582	Peak 3: 0.00	0.0	0.00
Result quality See result quality report			



	Mean (mV)	Area (%)	St Dev (mV)
Zeta Potential (mV): -25.1	Peak 1: -21.6	96.0	5.26
Zeta Deviation (mV): 24.3	Peak 2: -2.13	4.0	3.34
Conductivity (mS/cm): 0.745	Peak 3: 0.00	0.0	0.00
Result quality See result quality report			





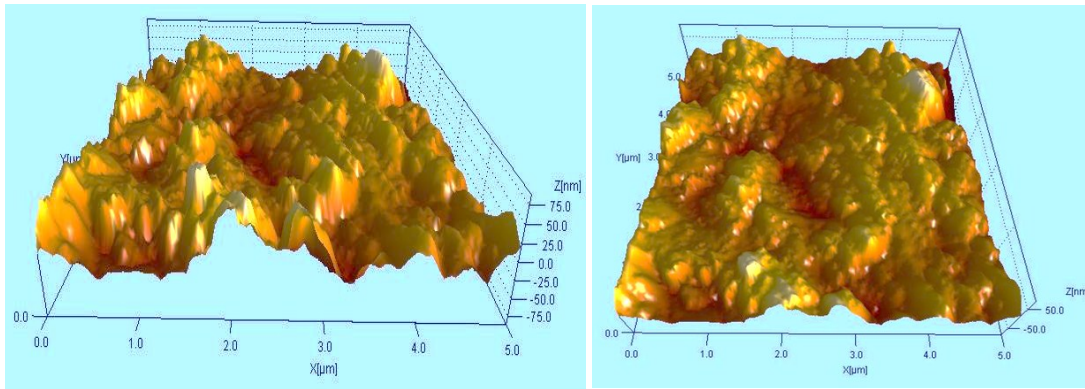


Fig. S1. **A)** FT-IR spectra of the GQDs (A) and CS-GQDs (B). **B)** The DLS curves of the GQDs (C) and CS-GQDs (D). **C)** Zeta potential diagram of the GQDs (E) and CS-GQDs (F). **D)** XRD diagram of the GQDs (G) and CS-GQDs (H). **E)** AFM image of the GQDs and CS-GQDs.

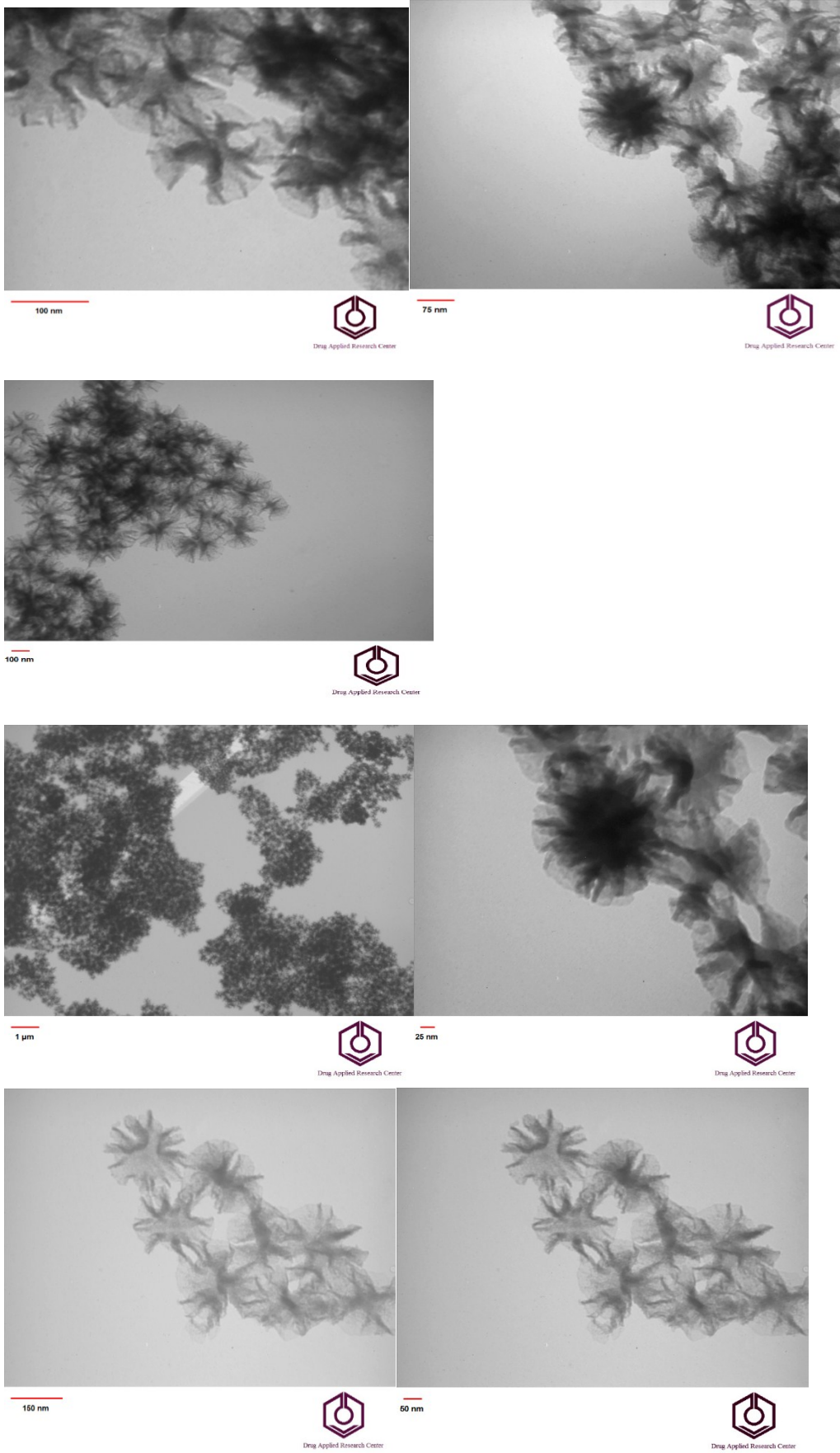
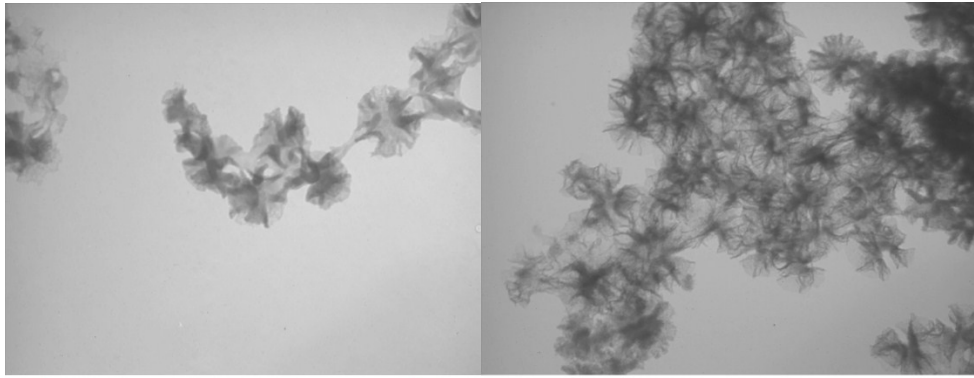


Fig. S2A



100 nm

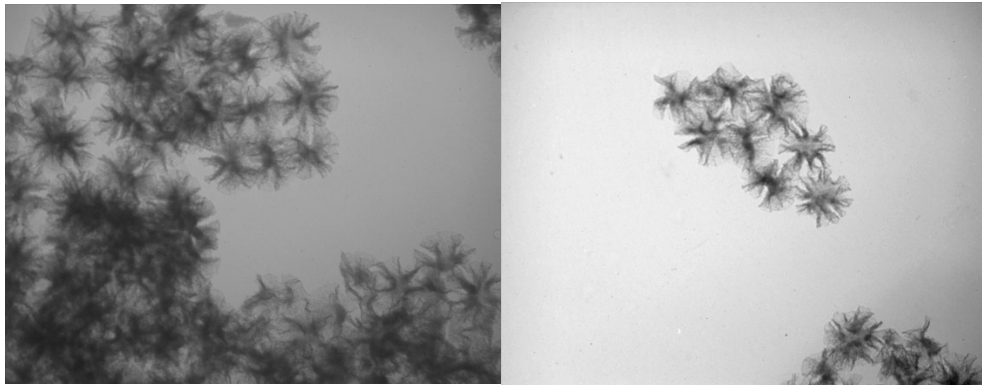


Drug Applied Research Center

150 nm



Drug Applied Research Center



50 nm



Drug Applied Research Center

100 nm



Drug Applied Research Center

Fig. S2B

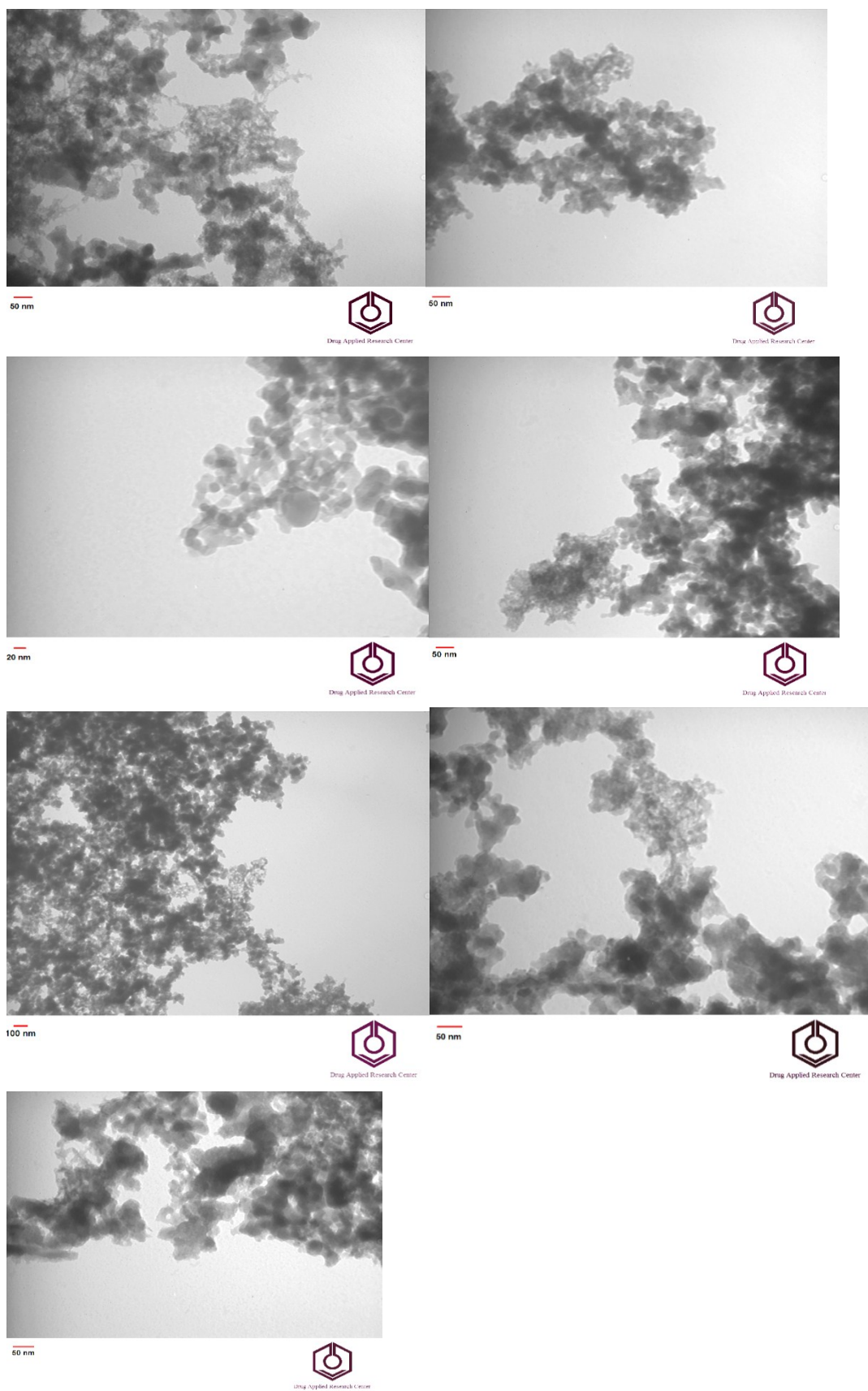


Fig. S2C

Fig. S2. **A)** The TEM images of the KCC-1. **B)** The TEM images of the KCC-1-NH₂. **C)** TEM images of the KCC-1-NH₂-Tb.

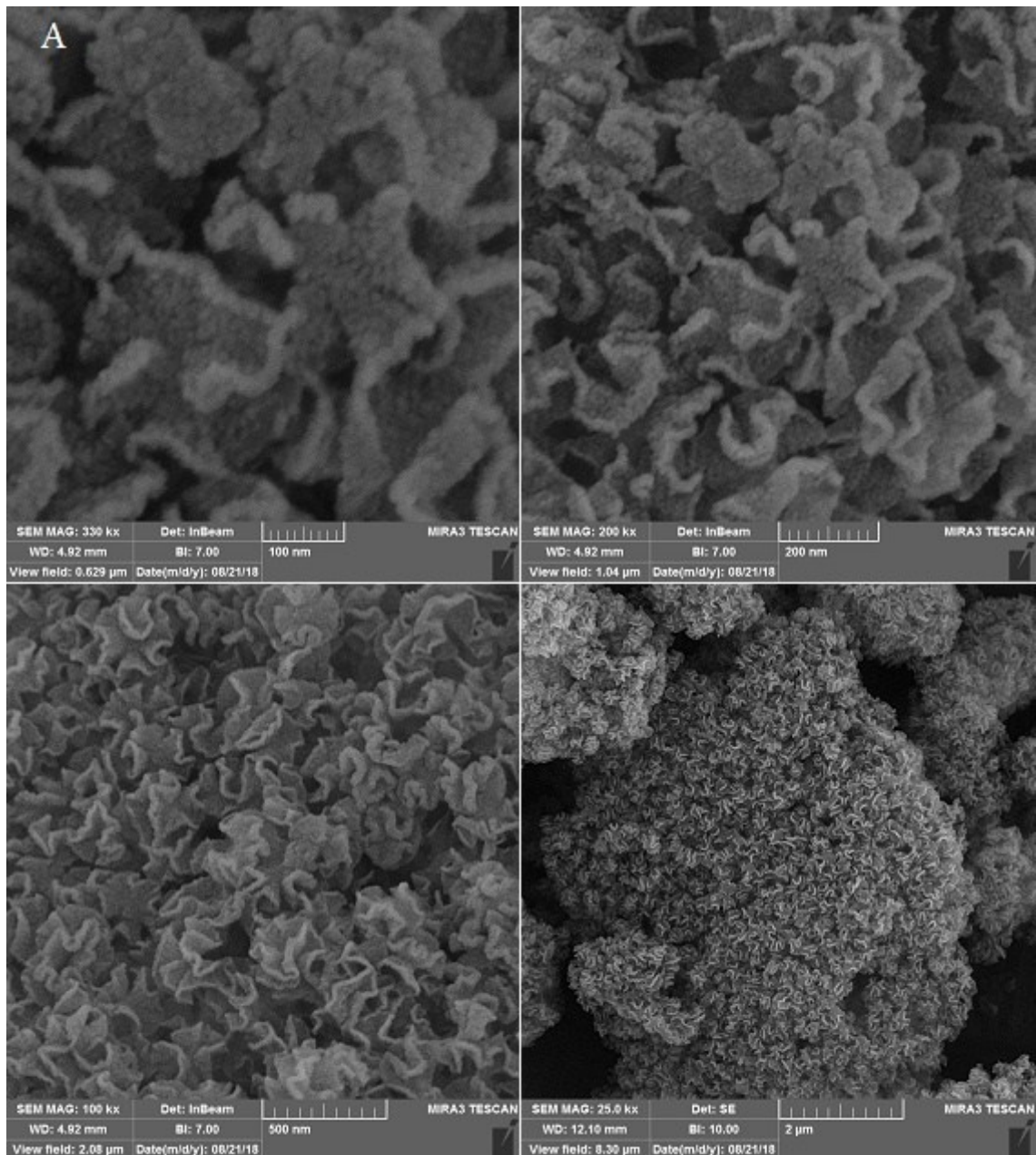


Fig.S3A

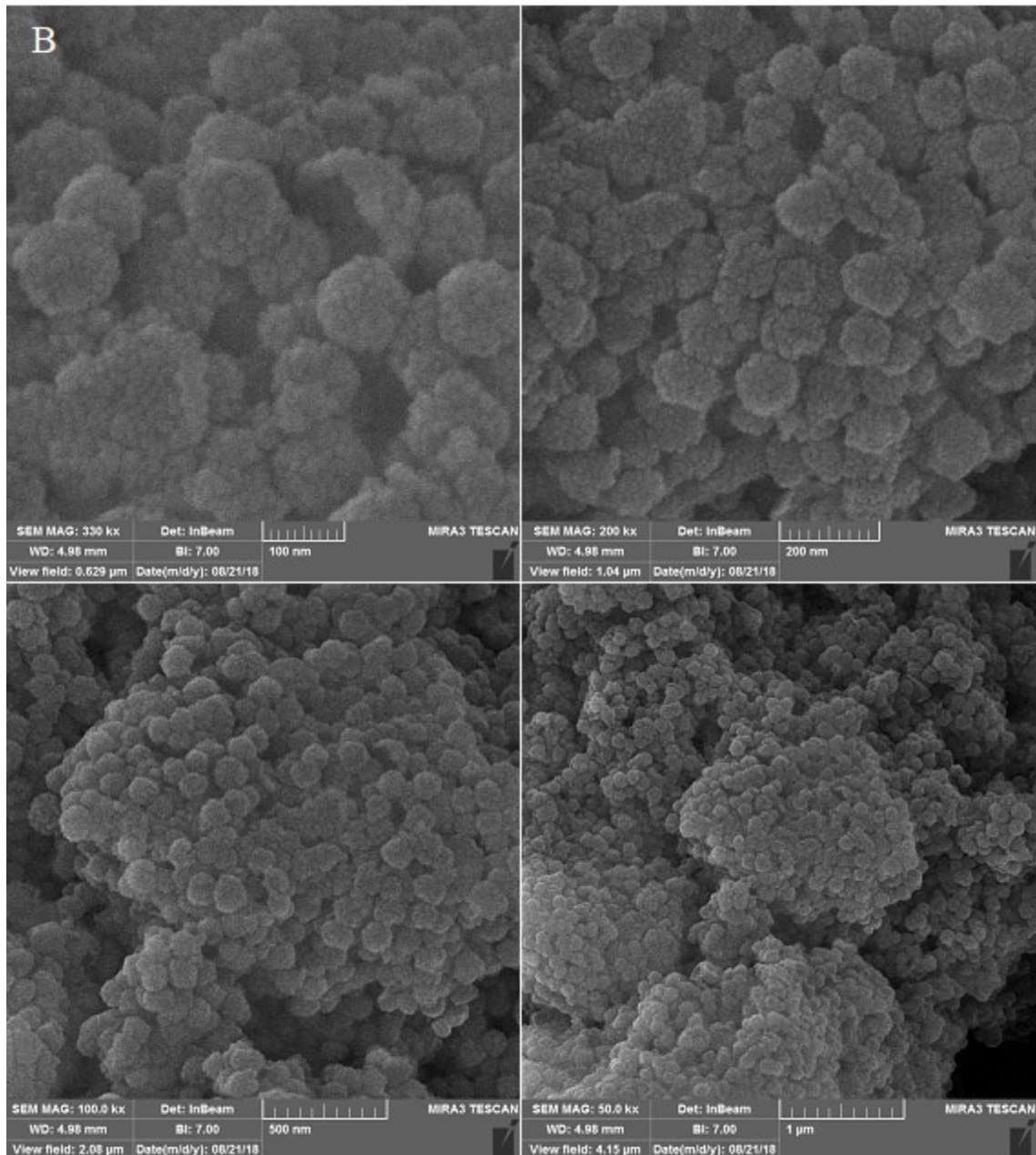


Fig. S3B

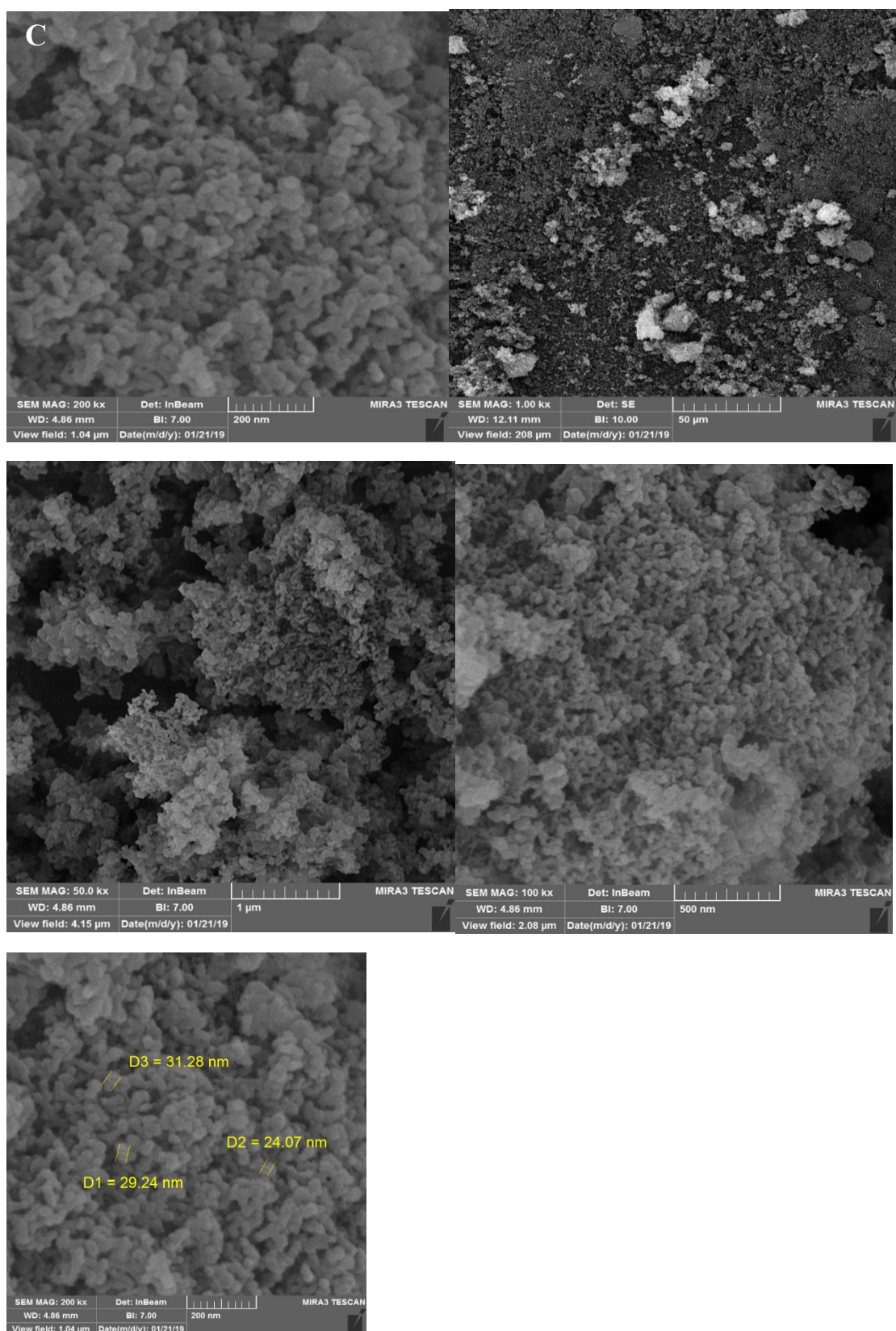


Fig. S3C

Fig. S3. FE-SEM images of the A) KCC-1. B) KCC-1-NH₂. C) KCC-1-NH₂-Tb in different magnification.

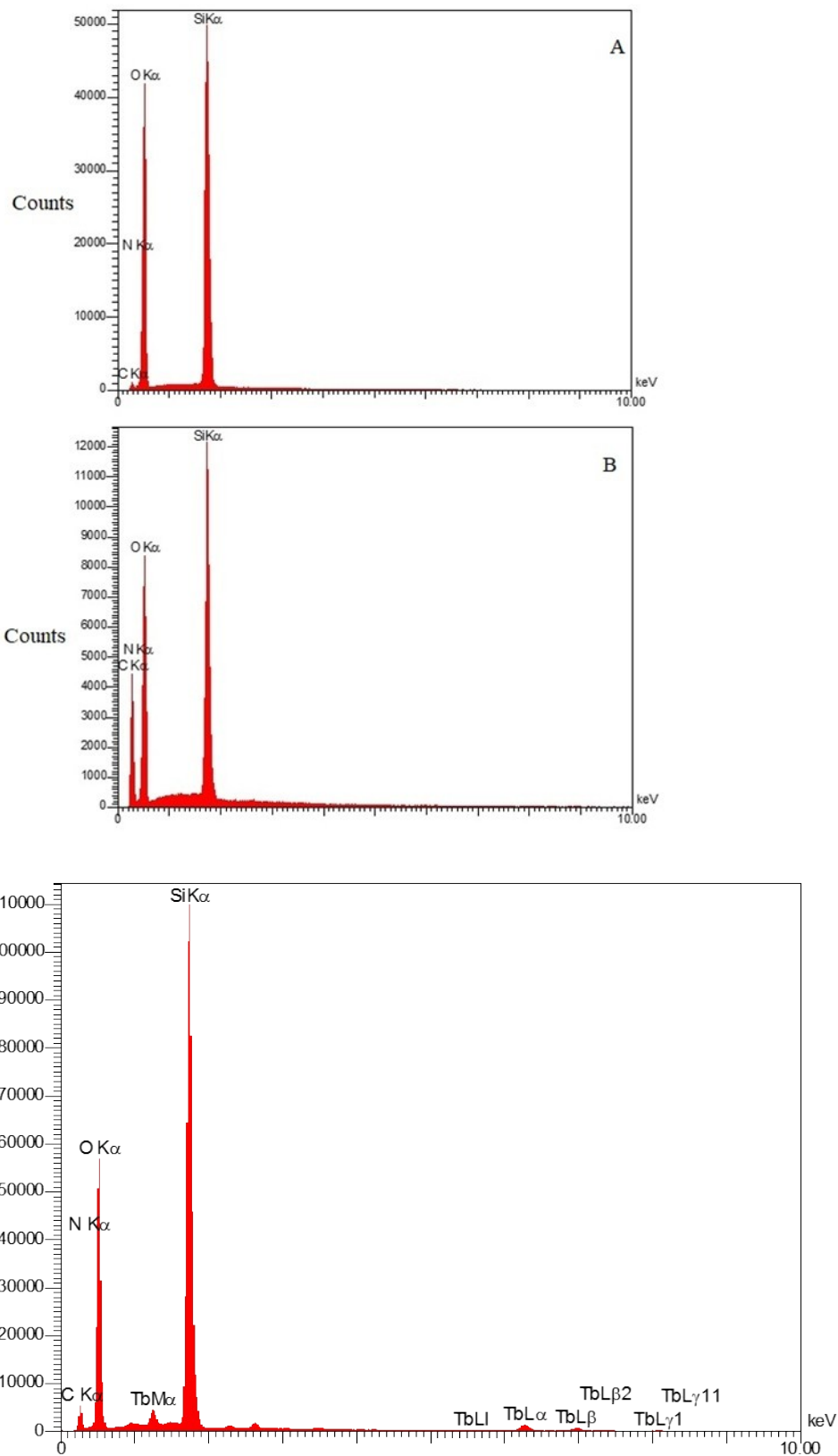


Fig. S4. EDS spectra of KCC-1 (A), KCC-1-NH₂ (B) and KCC-1-NH₂-Tb (C).

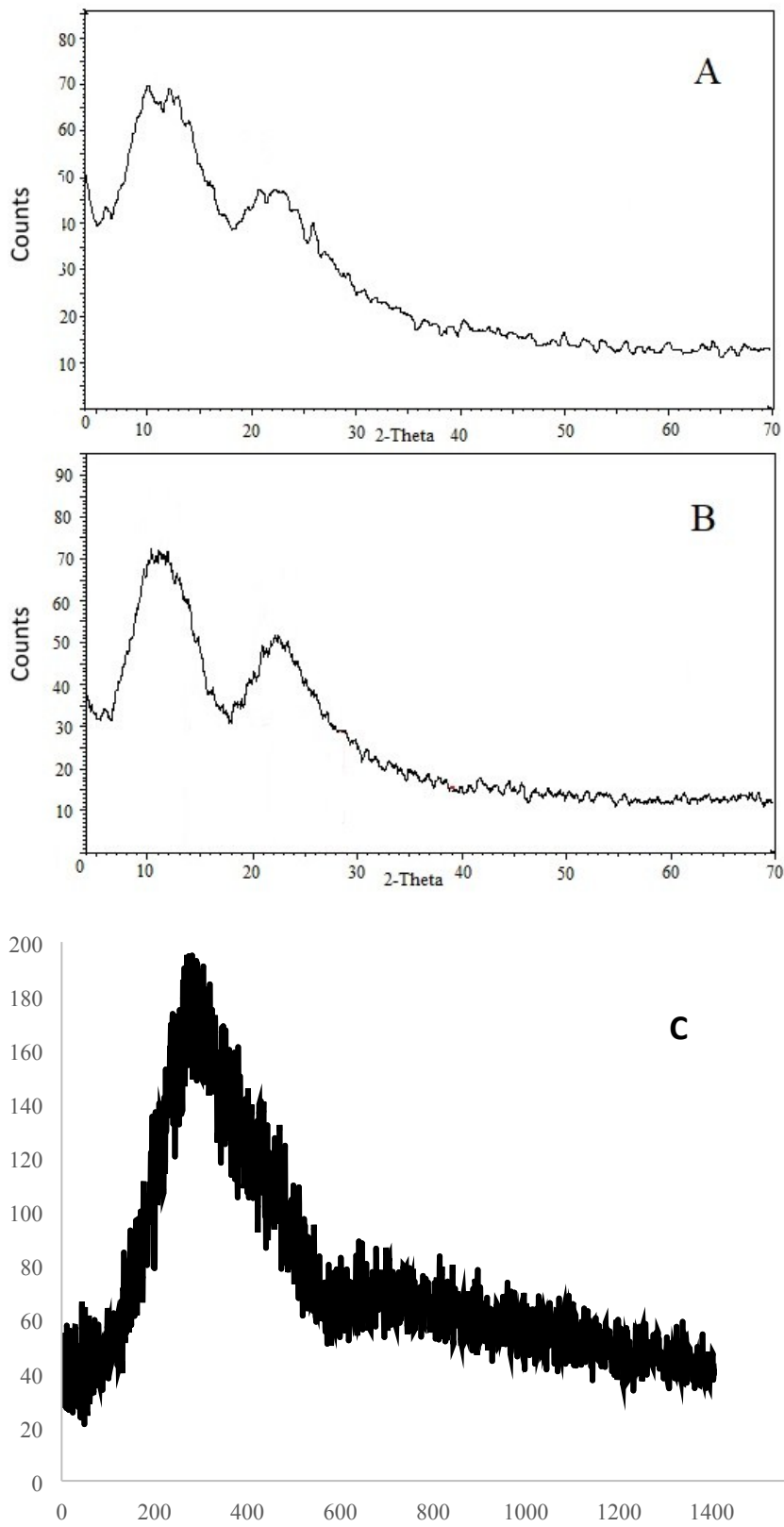


Fig. S5. XRD analysis of KCC-1 (A), KCC-1-NH₂ (B) and KCC-1-NH₂-Tb (C).

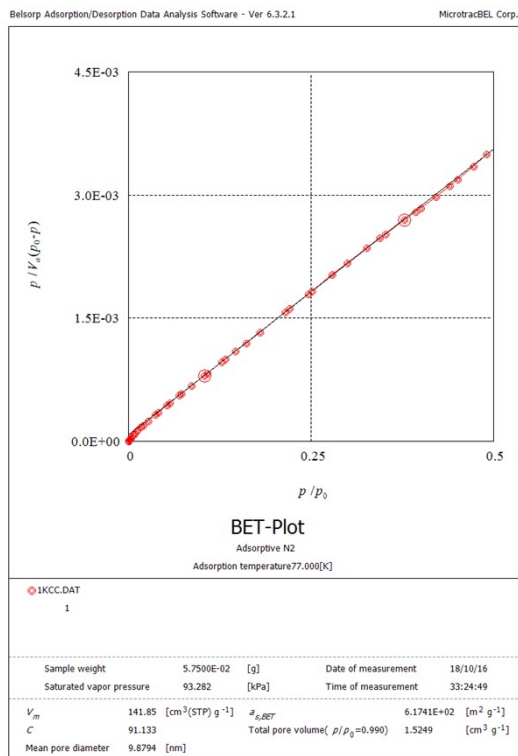
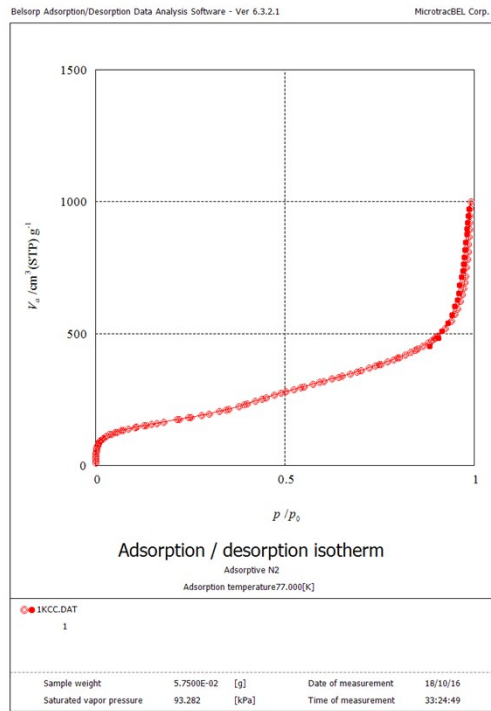
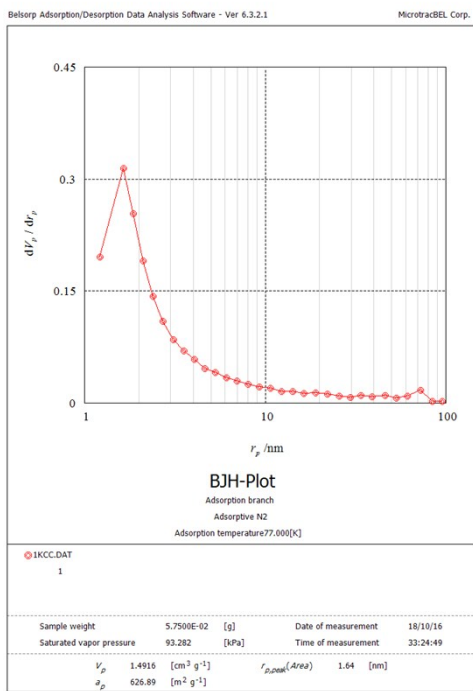


Fig. S6A

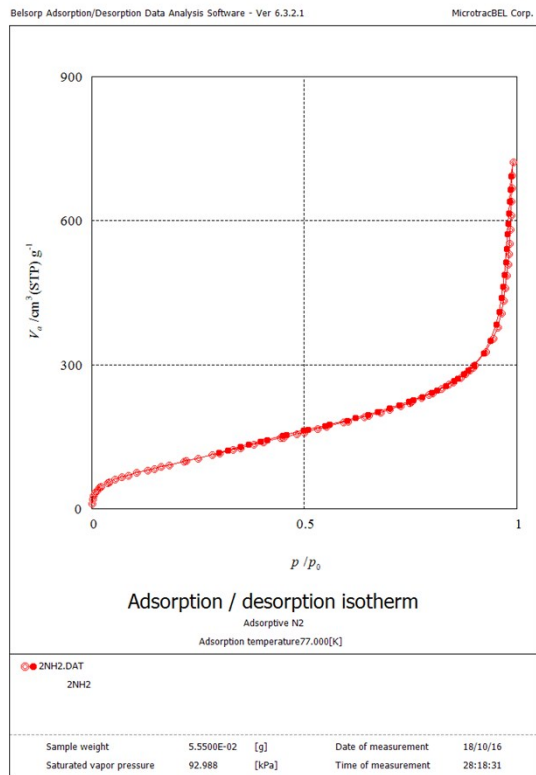
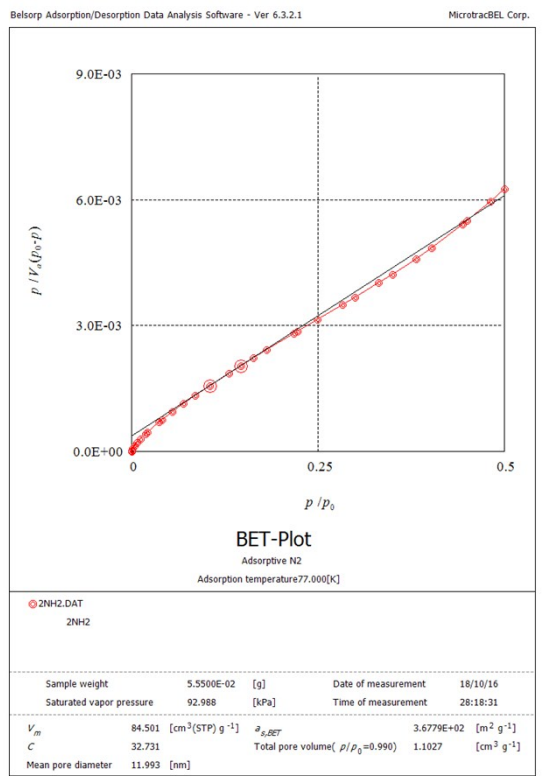
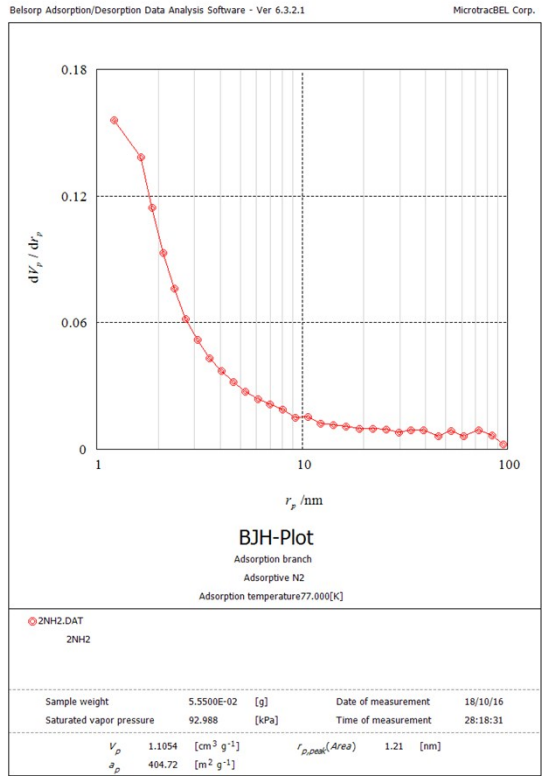


Fig. S6B

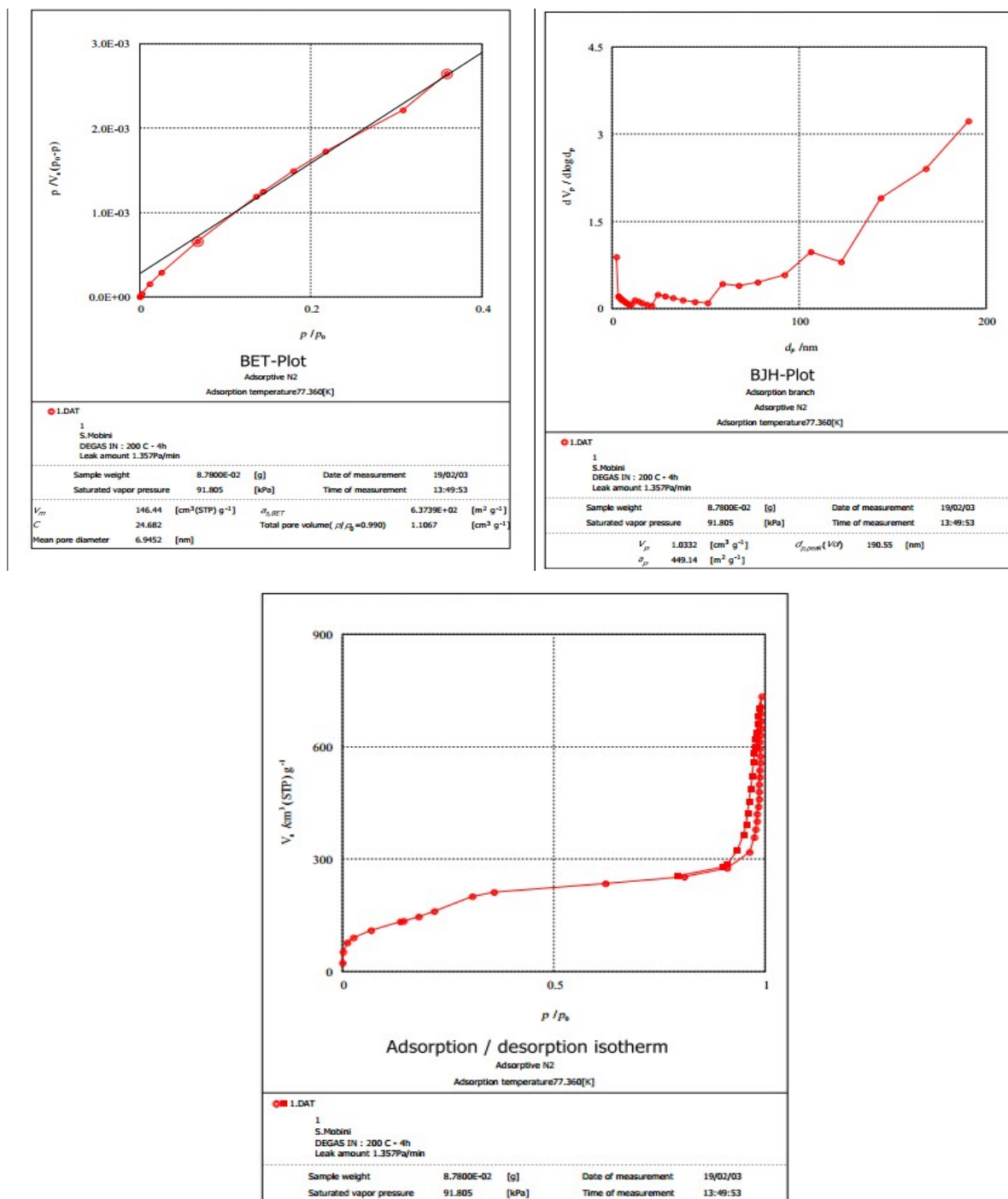


Fig. S6C

Fig. S6. BET pattern of **A)** KCC-1. **B)** KCC-1-NH₂. **C)** KCC-1-NH₂-Tb. The nitrogen adsorption-desorption isotherms and BET surface areas were measured at 77.360 K using BELSORP-mini II analysis program.

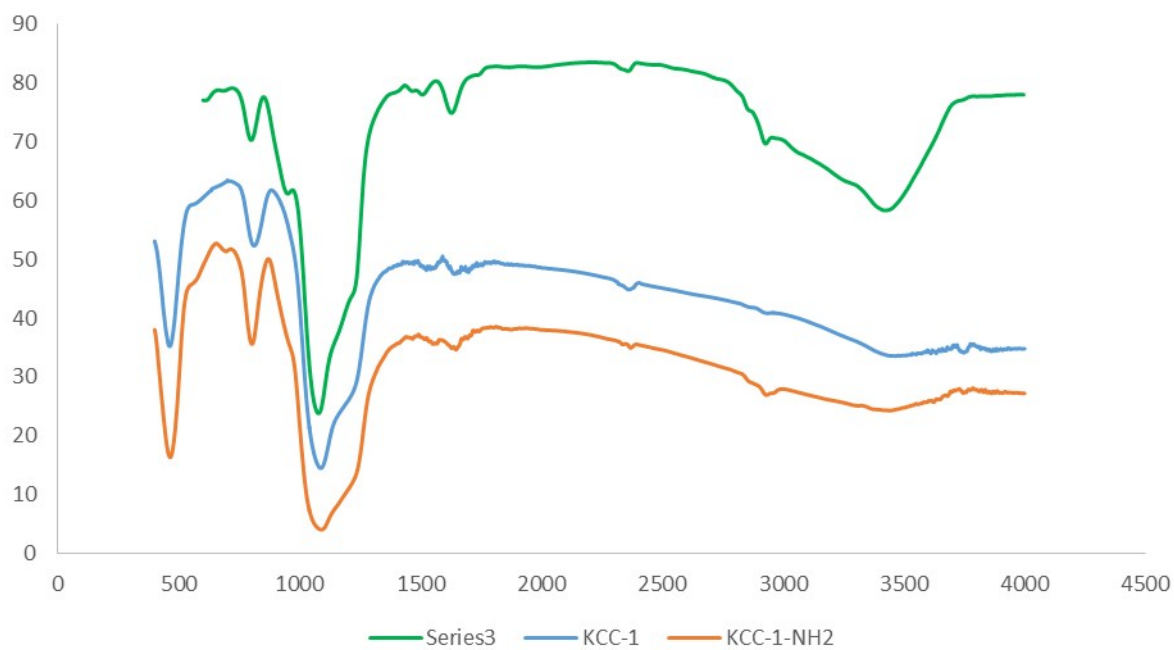


Fig. S7. FT-IR analysis of the KCC-1, KCC-1-NH₂ and KCC-1-NH₂-Tb.

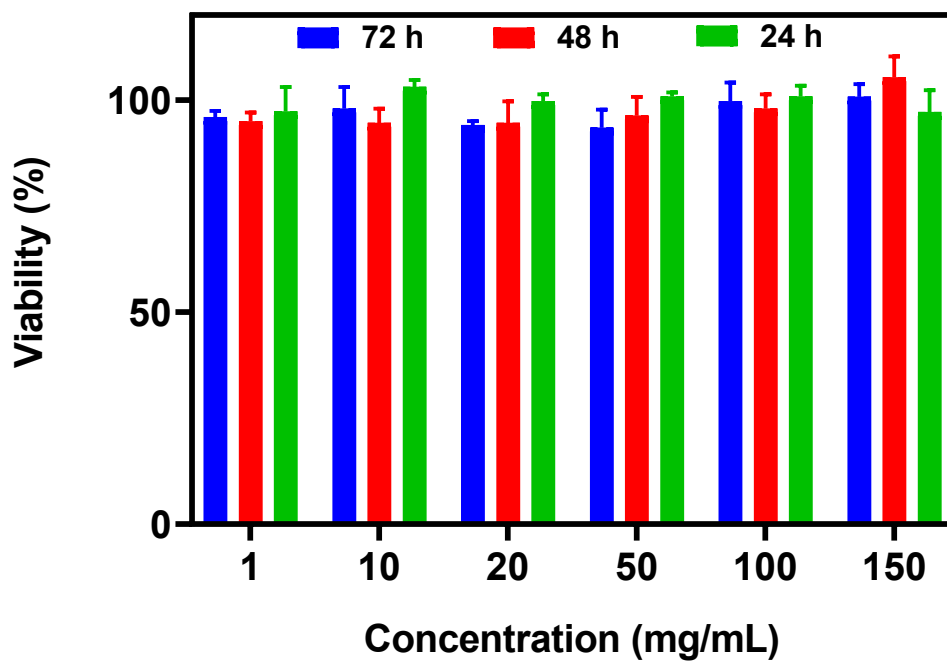
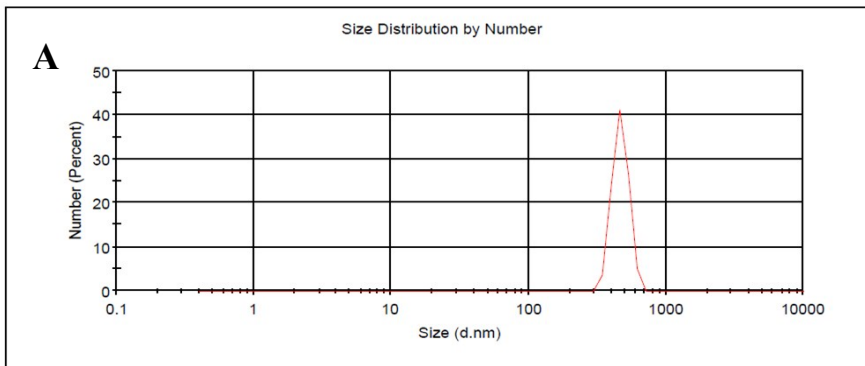


Fig. S8. MTT test result of the KCC-1-NH₂-Tb.

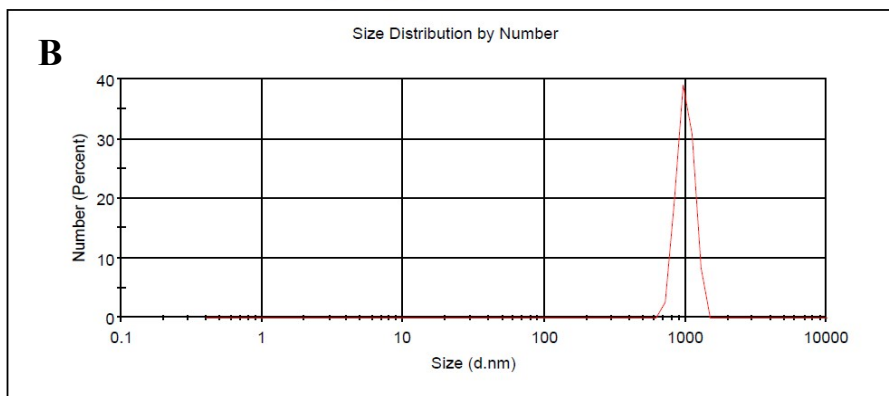
	Size (d.n...	% Number:	St Dev (d.n...
Z-Average (d.nm): 1074	Peak 1: 466.8	100.0	63.28
Pdl: 0.868	Peak 2: 0.000	0.0	0.000
Intercept: 0.974	Peak 3: 0.000	0.0	0.000

Result quality Refer to quality report



	Size (d.n...	% Number:	St Dev (d.n...
Z-Average (d.nm): 2006	Peak 1: 997.7	100.0	137.8
Pdl: 0.320	Peak 2: 0.000	0.0	0.000
Intercept: 1.04	Peak 3: 0.000	0.0	0.000

Result quality Refer to quality report



	Size (d.n...	% Number:	St Dev (d.n...
Z-Average (d.nm): 1022	Peak 1: 588.8	100.0	106.4
Pdl: 0.601	Peak 2: 0.000	0.0	0.000
Intercept: 1.01	Peak 3: 0.000	0.0	0.000

Result quality Refer to quality report

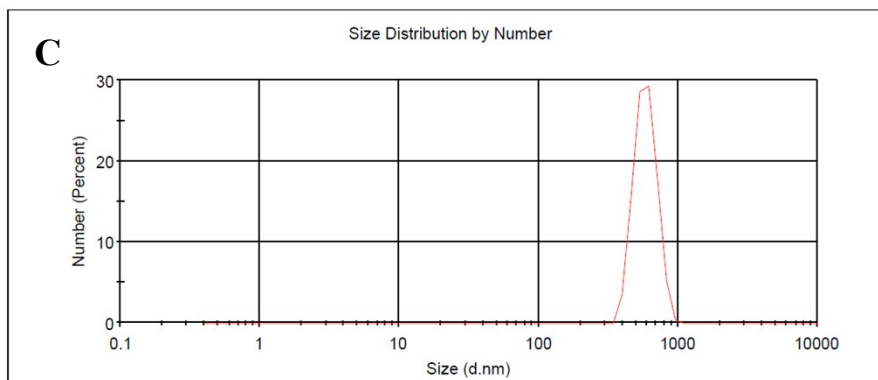


Fig. S9. DLS diagram of the KCC-1 (A), KCC-1-NH2 (B) and KCC-1-NH2-Tb (C).

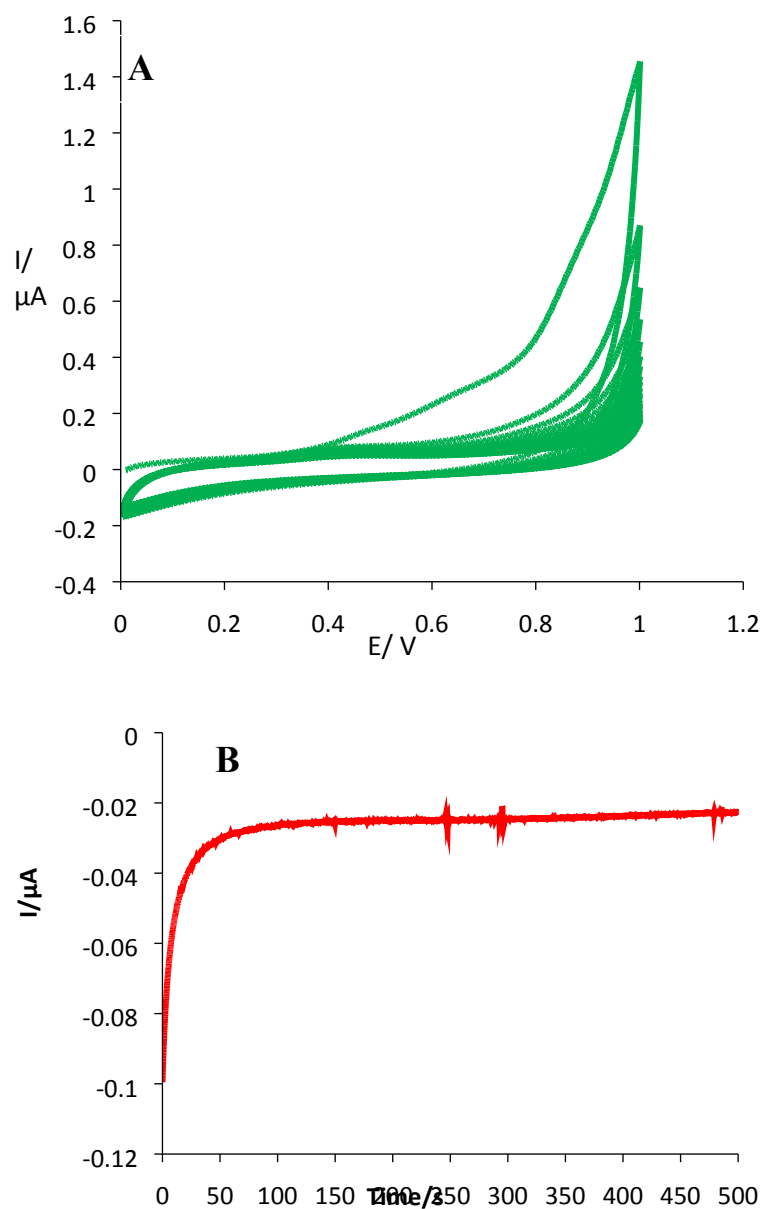
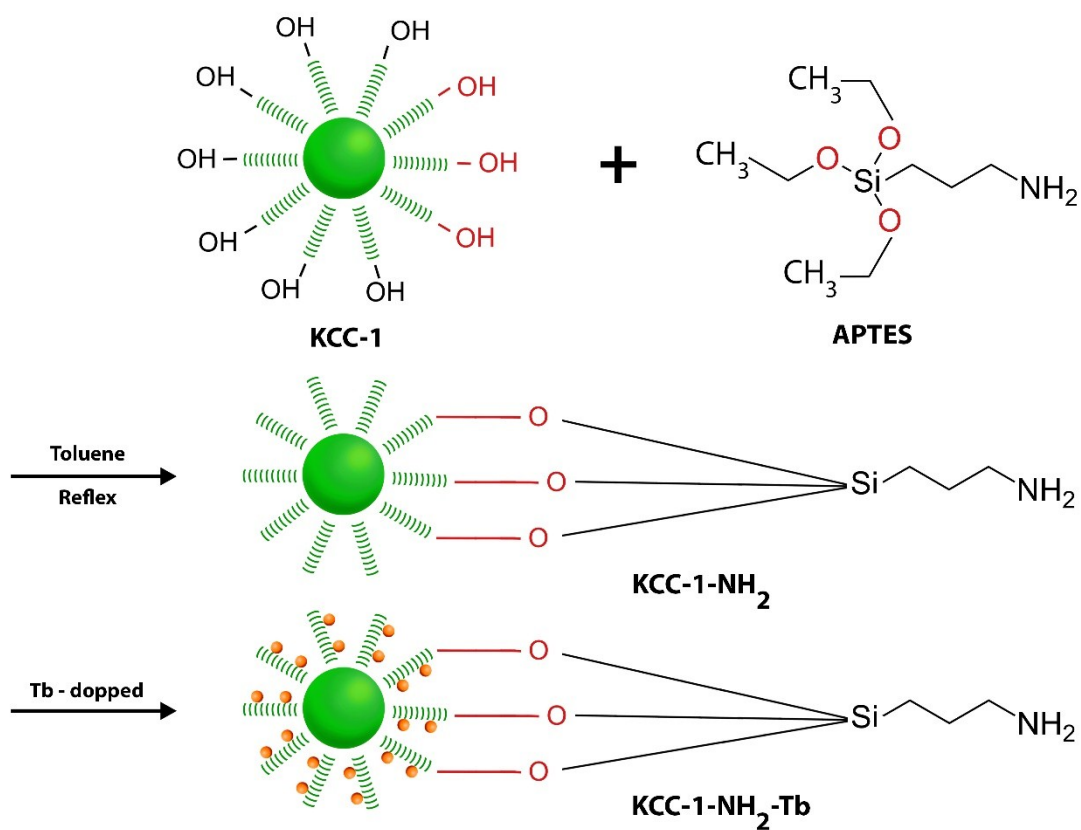


Fig. 10. **A)** The electrochemical deposition of CS-GQDs on the surface of glassy carbon electrode and that was carry out with 30 successive cycles in the range of 0 to +1 V with scan rate of 0.1 V/s. **B)** The electrodeposition of KCC-1-NH₂-Tb on the surface of CS-GQDs by chronoamperometry techniques at $E=-0.24\text{V}$ and duration time of 500 s.



Scheme S1: Synthesis procedure of KCC-1-NH₂-Tb

Table S1. Surface area, average pore size, and pore volume of KCC-1, KCC-1-NH₂ and KCC-1-NH₂-Tb.

Material type	Pore size (nm) ^a	Pore volume (cm ³ g ⁻¹) ^b	Surface Area (m ² g ⁻¹)
KCC-1	9.9	1.50	617
KCC-1-NH ₂	11.9	1.10	367
KCC-1-NH ₂ -Tb	6.94	1.06	633

^a Pore size was calculated by BET. ^b Pore volume determined by BJH.

References

- [1] M. Hasanzadeh, N. Shadjou, M. Marandi. *J. Nanosci. Nanotech.* 2017, **17**, 4598-4607.
- [2] A.Mirzaie, M. Hasanzadeh, A. Jouyban. *Int. Journal of Biological Macromolecules.* 2019, **123**, 1091-1105
- [3] V. Polshettiwar, D. Cha, X. Zhang, J.M Basset. *Angewandte Chemie.* 2010, **49**, 9652-9656
- [4] S. M. Sadeghzadeh, R. Zhiani, M. Khoobi, S. Emrani. *J. Microporous Mesoporous Mater.* 2018, **257**, 147-153
- [5] RC. Engstrom. *Anal. Chem.y.* 1982, **54**, 242310–242314.